Cellular automata designed for simulation of films growth

Krzysztof Malarz

http://home.agh.edu.pl/malarz/

Faculty of Physics & Applied Computer Science

AGH University of Science & Technology

Kraków, Poland

1 Introduction [1]

MBE = growth of an oriented single-crystal film of one material upon a single-crystal substrate of another when the main microscopic process is particles deposition followed by their diffusion on the surface — may be grouped to continuum and discrete approaches

2 Cellular automata (CA) [2]

- large lattice of sites
- each site carries an discrete information
- a state of site at time $t+1$ depends on their own and their neighbours states at time t

CA = network + set of site's states + rule of game

3 Surface characteristics

- film height $h(\vec{r},t)$ with θ on average
- height-height correlation function

$$G(\vec{s}) \equiv \langle h(\vec{r}+\vec{s})h(\vec{r})\rangle - \langle h(\vec{s})\rangle^2$$

- film roughness, i.e. surface width

$$\sigma \equiv \sqrt{G(\vec{0})}$$

- surface anisotropy

$$\varepsilon \equiv \frac{G(\hat{x}) - G(\hat{y})}{G(\vec{0})}, \qquad \varepsilon_1 \equiv \frac{\phi_x - \phi_y}{\phi_x + \phi_y},$$

$$\varepsilon_2 \equiv \phi_x / \phi_y, \qquad \varepsilon_3 \equiv \ell / A,$$

where ϕ_x and ϕ_y are x- and y-side of the minimal rectangle which totally covers whole cluster, ℓ is the cluster perimeter and A is the the cluster area.

- surface selfaffinity = surface shape and statistical properties are invariant when simultaneously

$$r \longrightarrow \lambda r$$

and

$$h(r) \longrightarrow \lambda^H h(r)$$

- dynamic Family–Vicsek scaling law [5]:

$$\sigma \propto L^{\alpha} f(\theta/L^{\gamma})$$

with

$$f(x) = \begin{cases} x^{\beta} & \text{for } x \ll 1, \\ 1 & \text{for } x \gg 1, \end{cases}$$

where L is linear size of substrate, α, β, γ are roughness, growth and dynamic exponent, respectively

$$\xi \propto L^{1/\gamma} \text{ and } \gamma = \alpha/\beta$$

- correlation length ξ
- before reaching $\theta_\infty \propto L^\gamma$ roughness grows like θ^β and then saturates on $\sigma_\infty \propto L^\alpha$.

4 Deterministic SOS models

solid-on-solid approximation (SOS): no overhangs or voids and surface may be fully characterised by a single-valued function $h(x,t)$

4.1 Random deposition model (RDM)

$T \to 0$, no diffusion

$$P(h;\theta) = \frac{\theta^h}{h!}\exp(-\theta); \quad \beta = 1/2; \quad \alpha = \infty$$

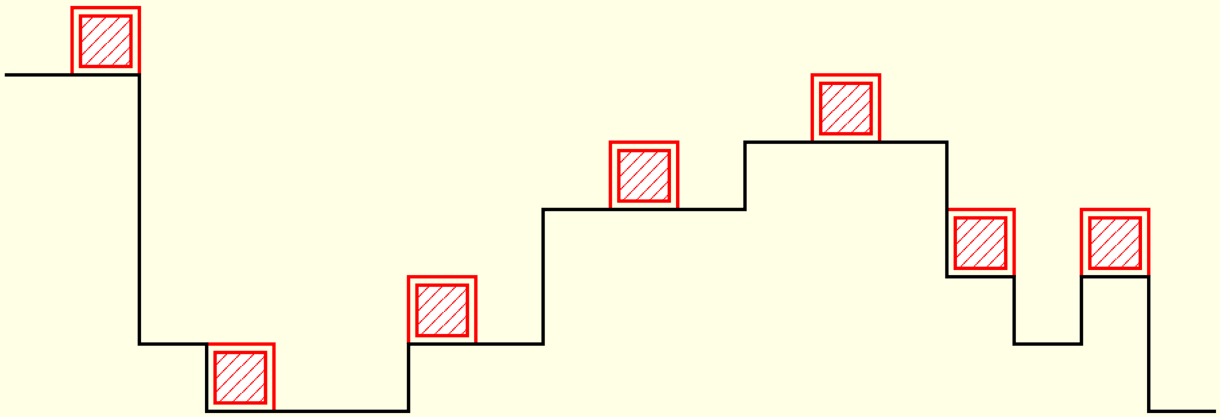

4.2 Family model [6]

RDM + surface diffusion to site with minimal height

$$h_{\text{min}} = \min\{h(r-R,t),\ldots,h(r+R,t)\}$$

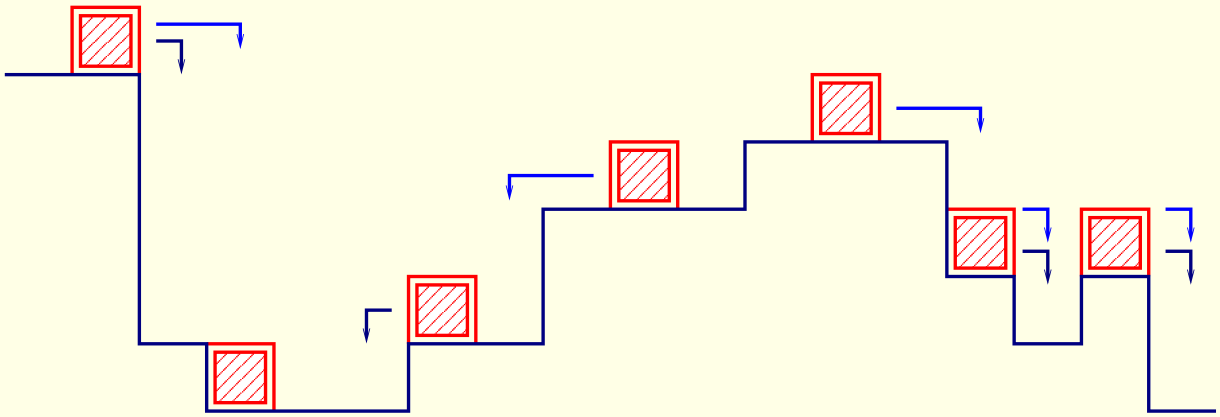

4.3 Das Sarma–Tamborenea model [7]

RDM + surface diffusion to a kink site

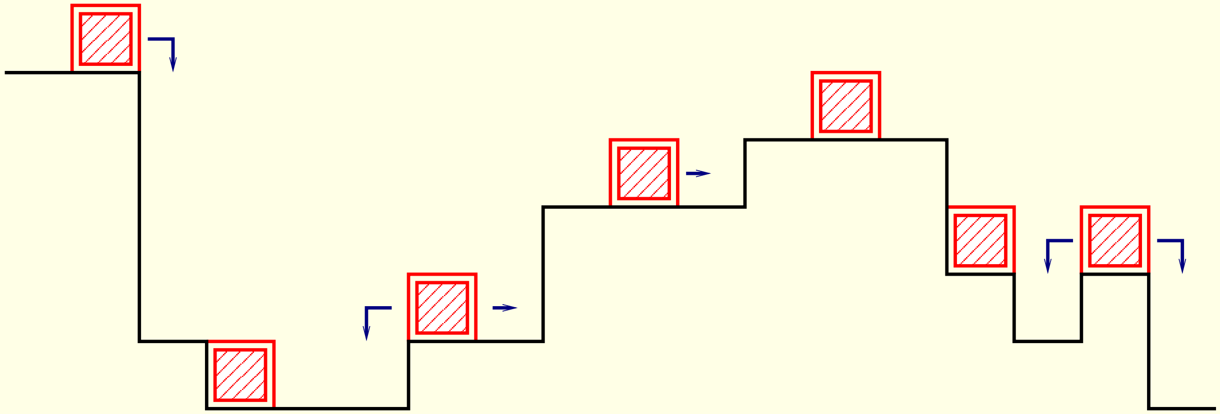

4.4 Wolf–Villain model [8]

RDM + surface diffusion to site with maximal z

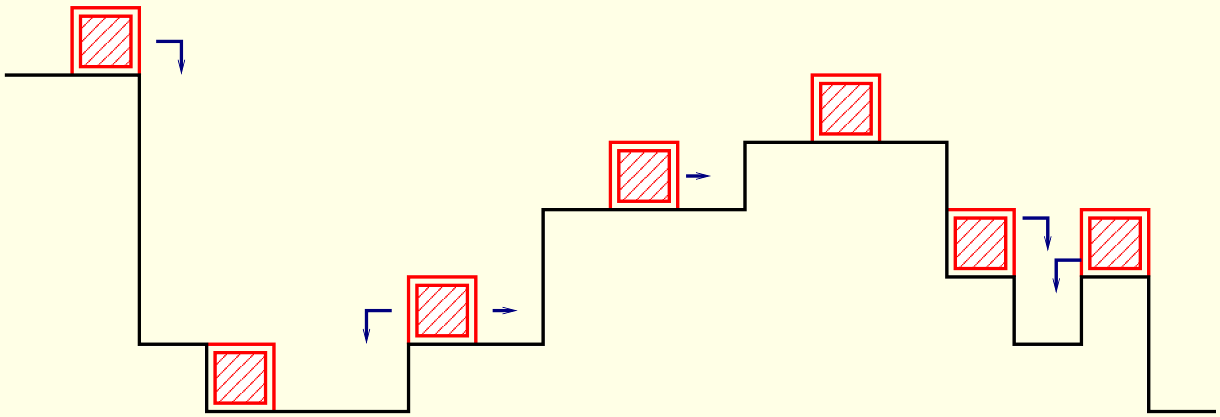

5 Probabilistic SOS models

before Arrhenius-like energy-activated full-reversible-diffusion kinetics model governed by diffusion constant $D = D_0 \exp(-E_a/k_B T)$ one may wish use probabilistic CA

CA rule involves tossing the coin

5.1 Adding substrate temperature

- binding energy at place of deposition and NN:

$$E_{i,j} = n_x^{i,j} J_x + n_y^{i,j} J_y + n_x^{i,j-1} S_x + n_y^{i,j-1} S_y.$$

- diffusion to one of NN with probability

$$P_i \propto \exp(-E_i / k_B T)$$

reduced by

$$\exp(V_x / k_B T) \text{ or } \exp(V_y / k_B T),$$

where V is diffusion barrier

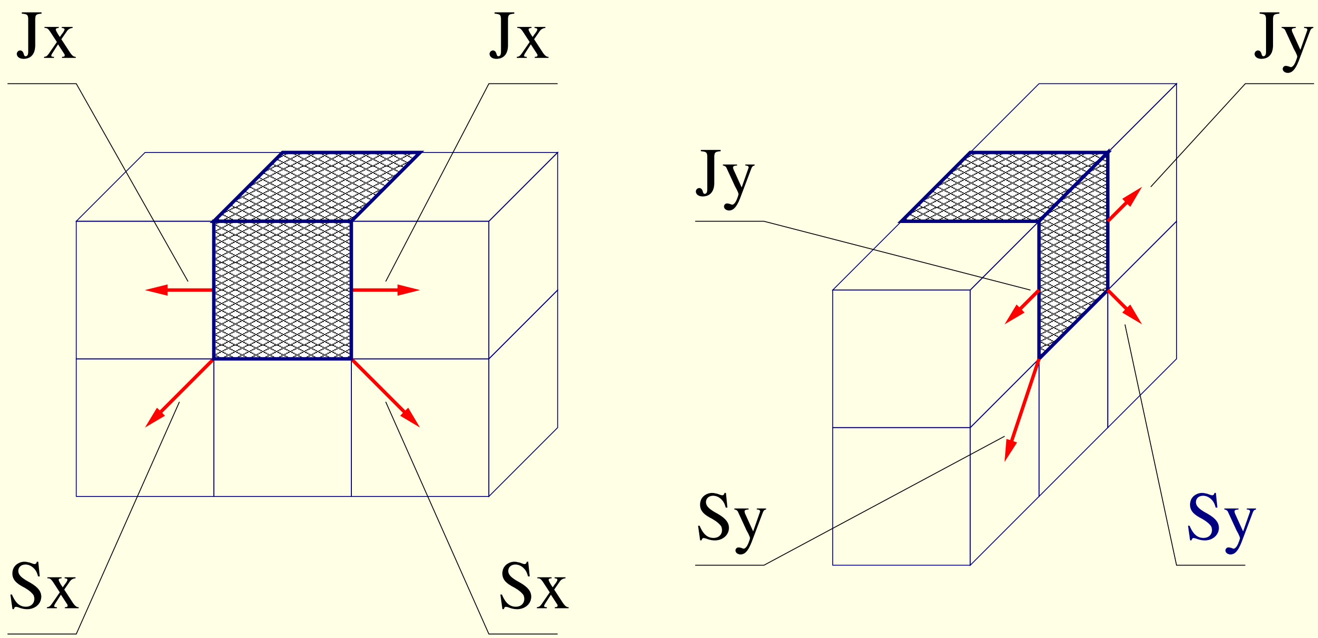

Figure 1: Model parameters S and J.

5.2 Toward Arrhenius-like kinetics [12]

- We start our simulation with perfectly flat substrate.

- Every τL^2 time steps new jet of $\theta_{\text{dep}} L^2$ particles arrives.

- Each time step — between subsequent acts of the depositions — particles 'sitting' on the column top may diffuse on the surface.

- The only mobile particles are those which currently have less than z_x and z_y created particle-particle lateral bonds (PPLB) in x-and y-direction, respectively.
- For isotropic case only one number z guards the particles mobility.
- Active particles and their movement directions are picked up randomly.

- The particles are not allowed to climb on higher levels, but they are able to jump down at the terrace edge.

- The simulation is carried out until a desired film thickness θ_{max} has been deposited.

6 Results

Here we show some results presented in Refs.

[9, 10, 11, 12]

6.1 Submonolayer growth [11]

- $\theta = 0.1$ [ML]
- anisotropy in E and V:

Ag: $V_x/V_y = 0.736, \quad E_x/E_y = 9.000$

Cu: $V_x/V_y = 0.793, \quad E_x/E_y = 6.857$

Influence of the substrate temperature on surface morphology:

- randomly deposited monomers
- long 1D chains
- larger 2D but still anisotropic clusters
- and again randomly deposited small atomic island

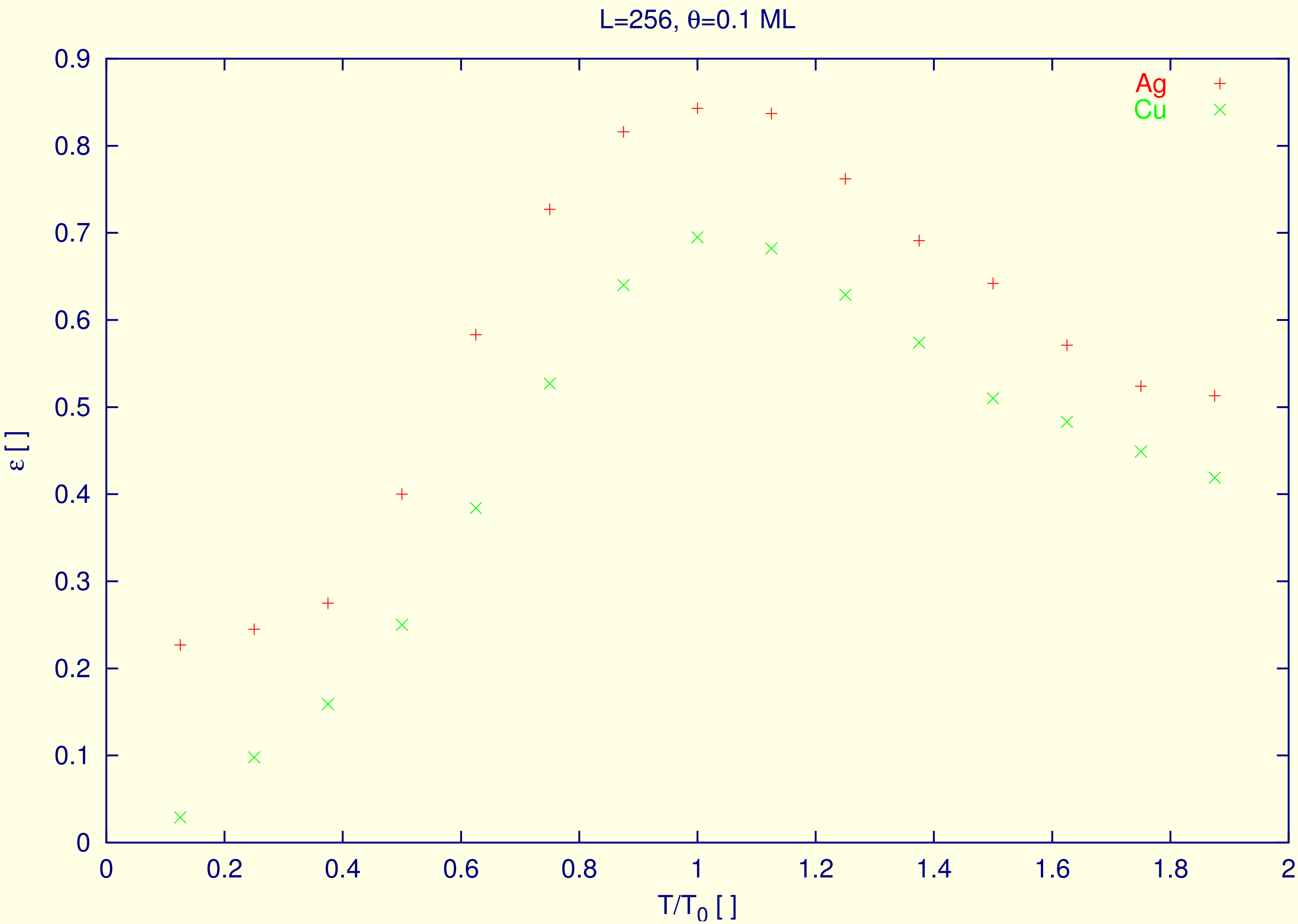

L=256, θ=0.1 ML
Ag
Cu
ε [ ]
T/T0 [ ]
0
0.1
0.2
0.3
0.4
0.5
0.6
0.7
0.8
0.9
0
0.2
0.4
0.6
0.8
1
1.2
1.4
1.6
1.8
2

6.2 Surface roughness [9, 12]

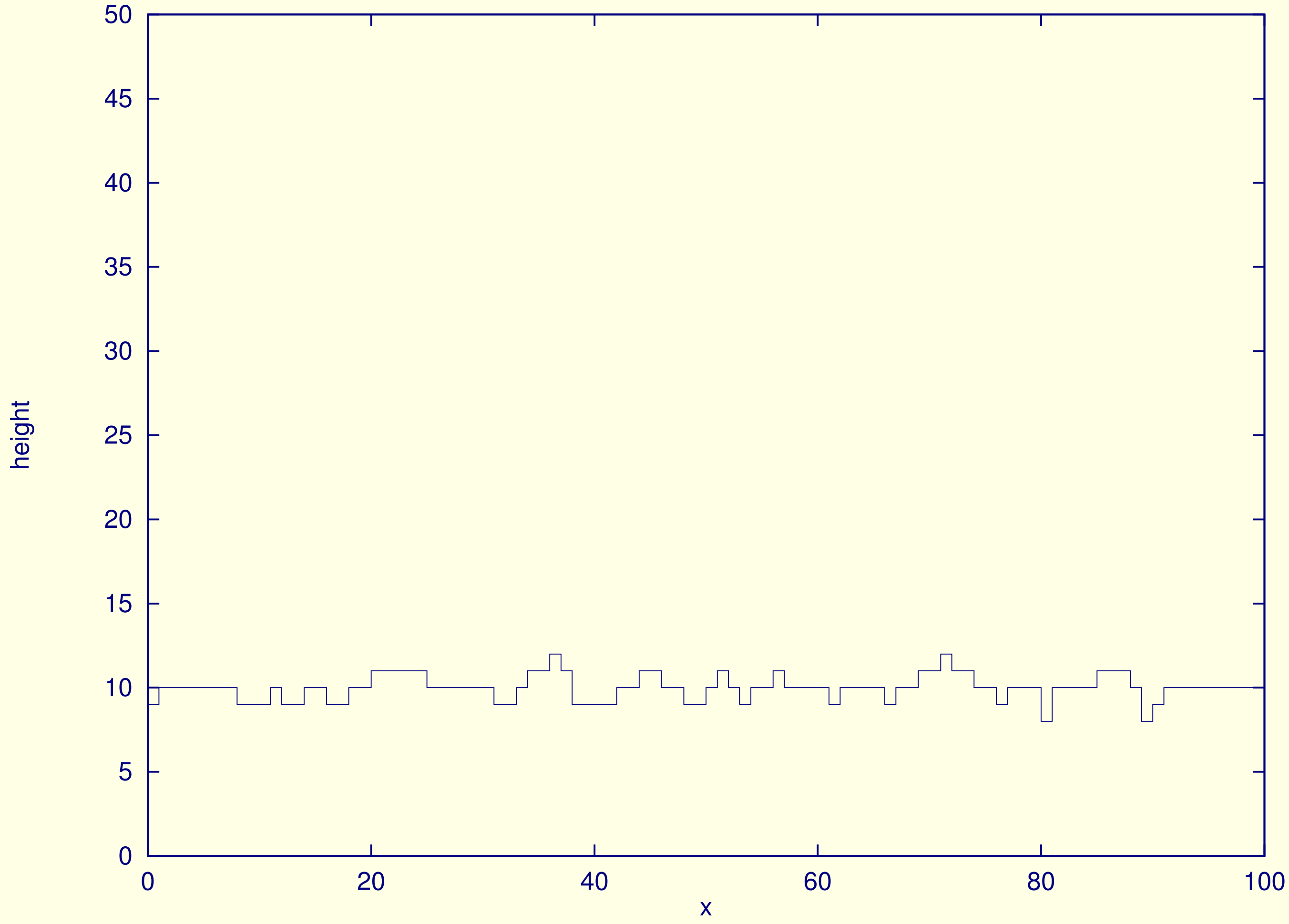

Figure 2: $J \to -\infty, V = 0, \langle h \rangle = 10$ [ML]

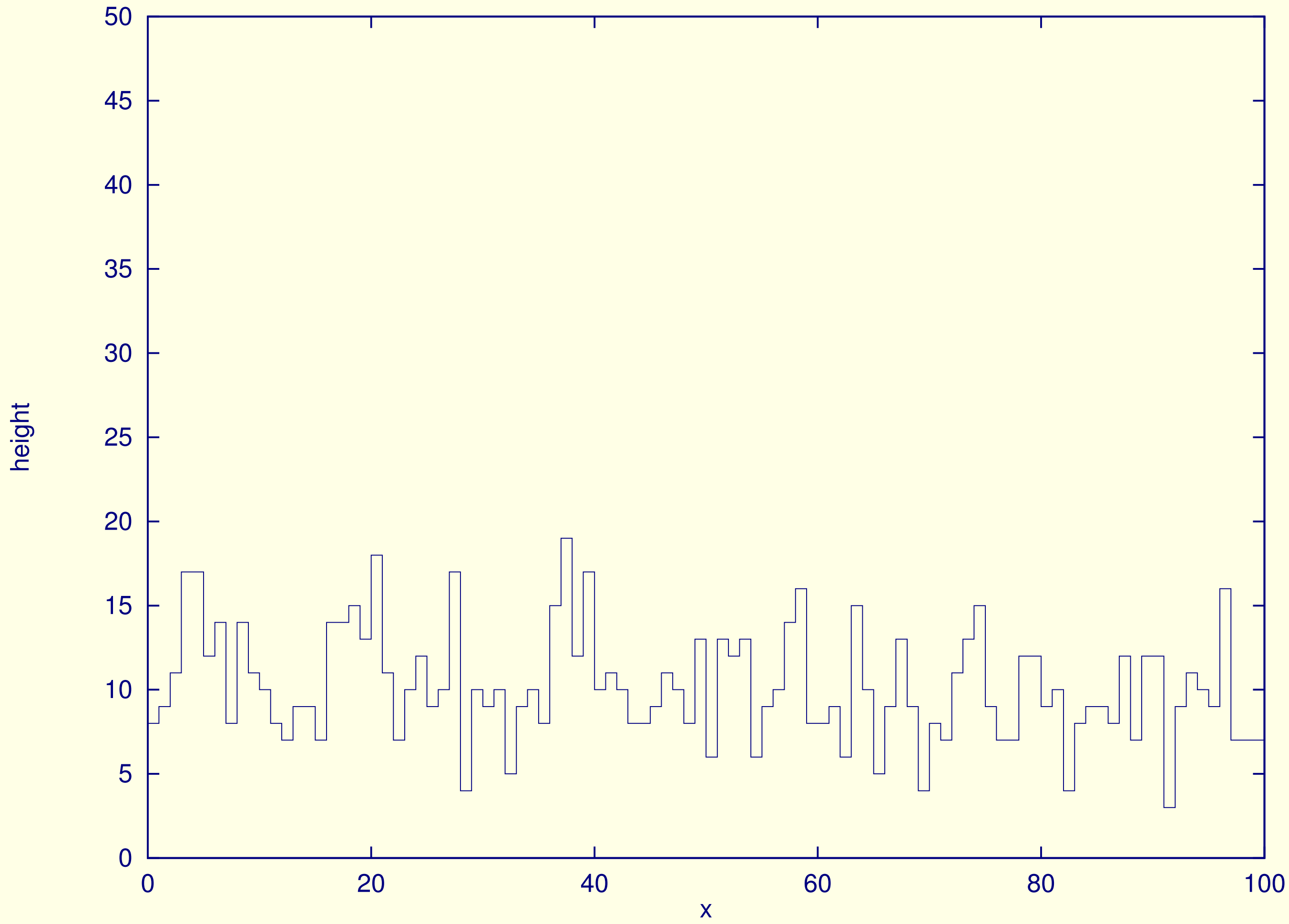

Figure 3: $J = 0, V \to \infty, \langle h \rangle = 10$ [ML]

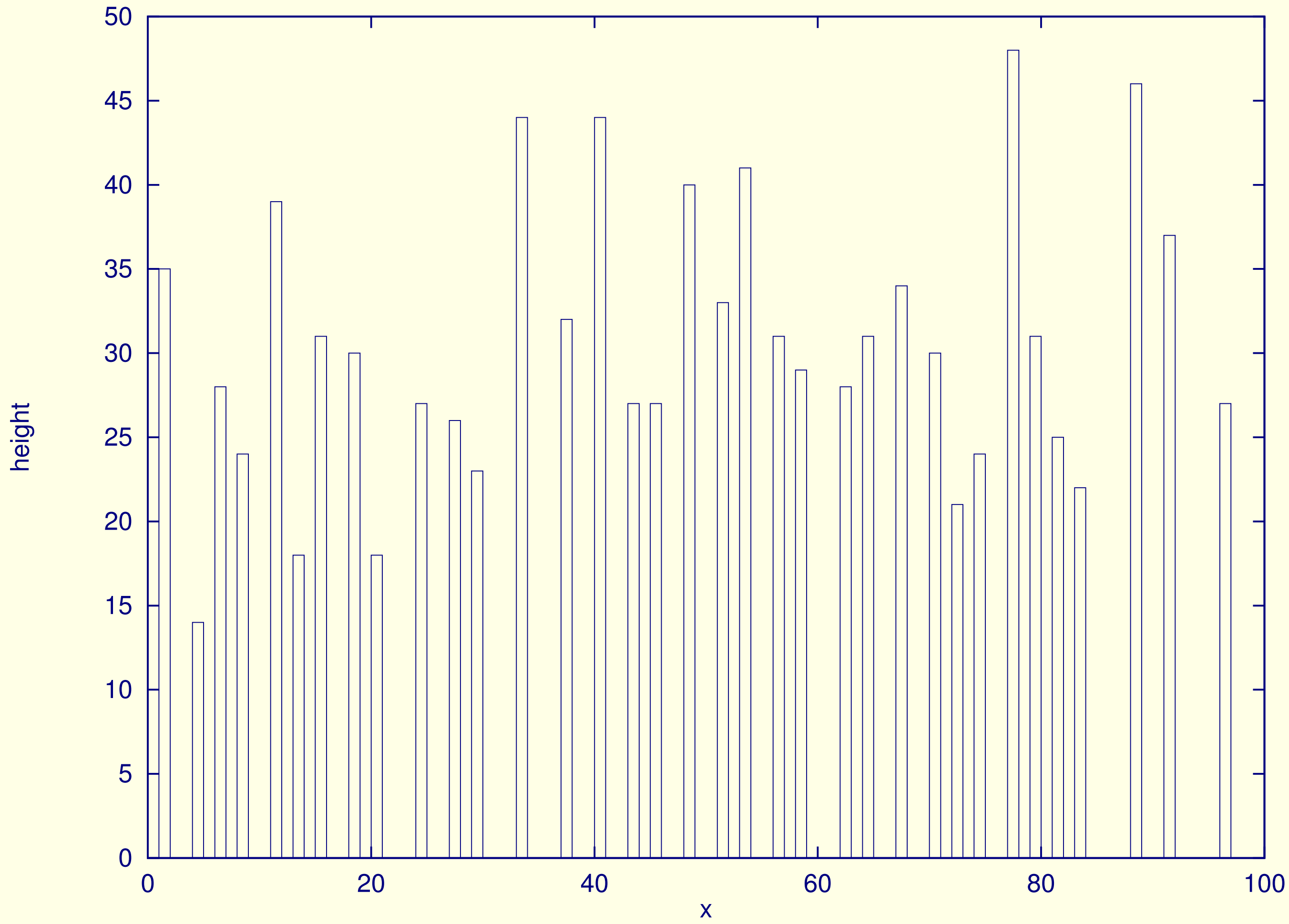

Figure 4: $J > 0, V = 0, \langle h \rangle = 10$ [ML]

$J \to -\infty$ and $V = 0 \to \alpha \approx 0.78$ and $\beta \approx 0.22$

Table 1: $\theta_{\text{dep}} = 0.1$ [ML], $\tau = 1$

z	1	2	3	4
α	0.863	0.215	0.1005	0.0718
β	0.357	0.123	0.0405	0.0228

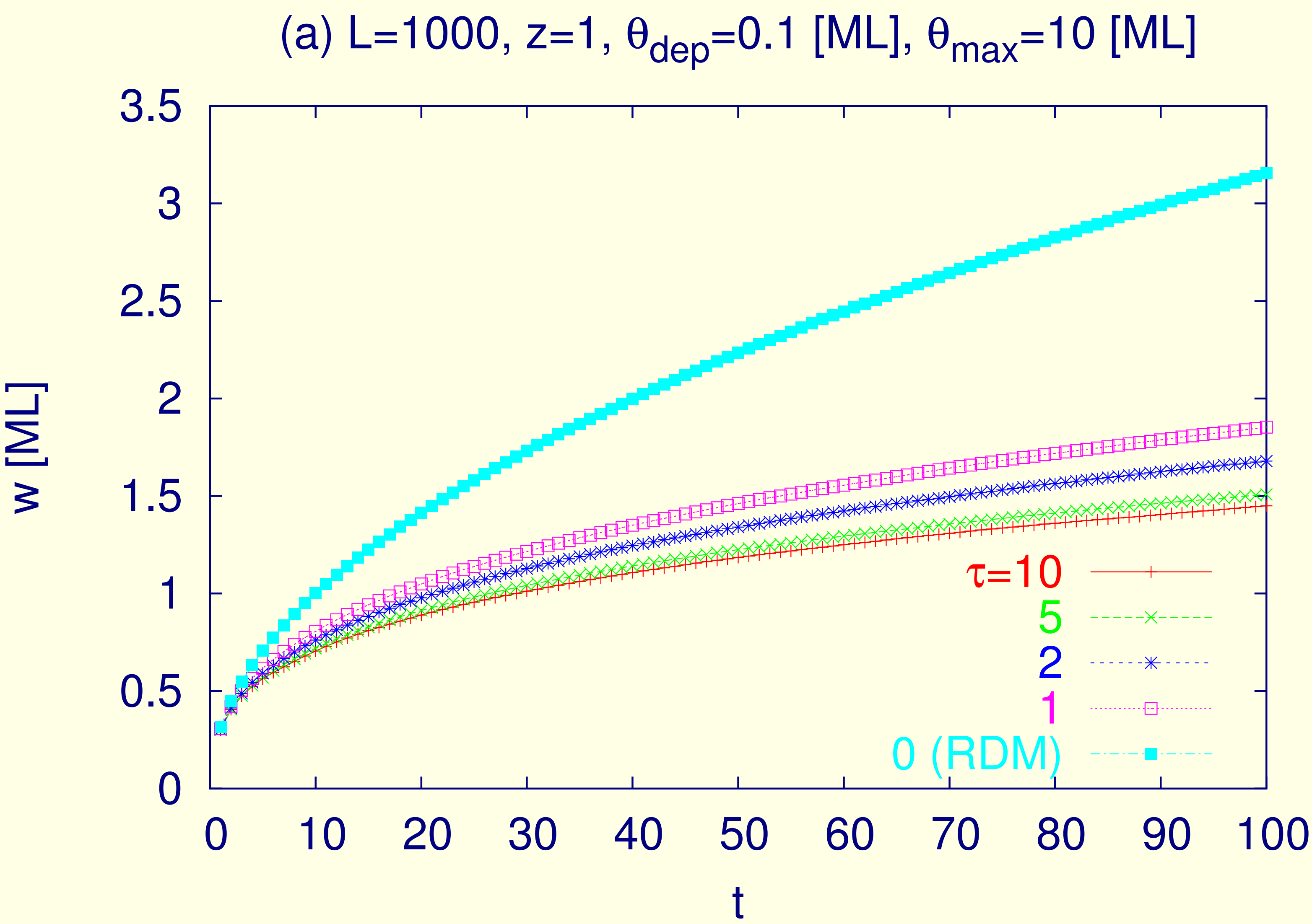

Figure 5: $z = 1$, $L = 10^3$, $\theta_{\rm dep} = 0.1$ [ML]

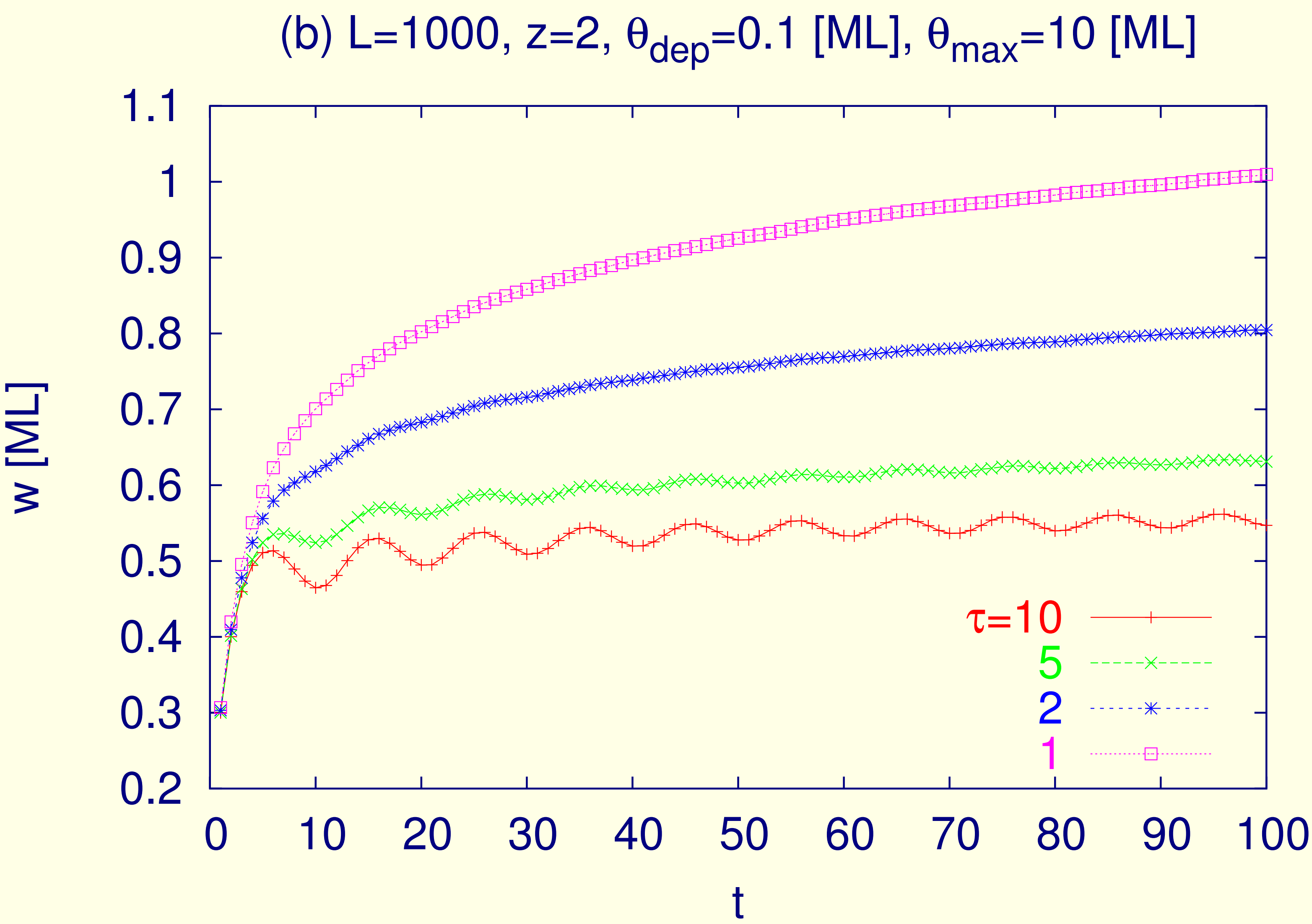

Figure 6: $z = 2$, $L = 10^3$, $\theta_{\text{dep}} = 0.1$ [ML]

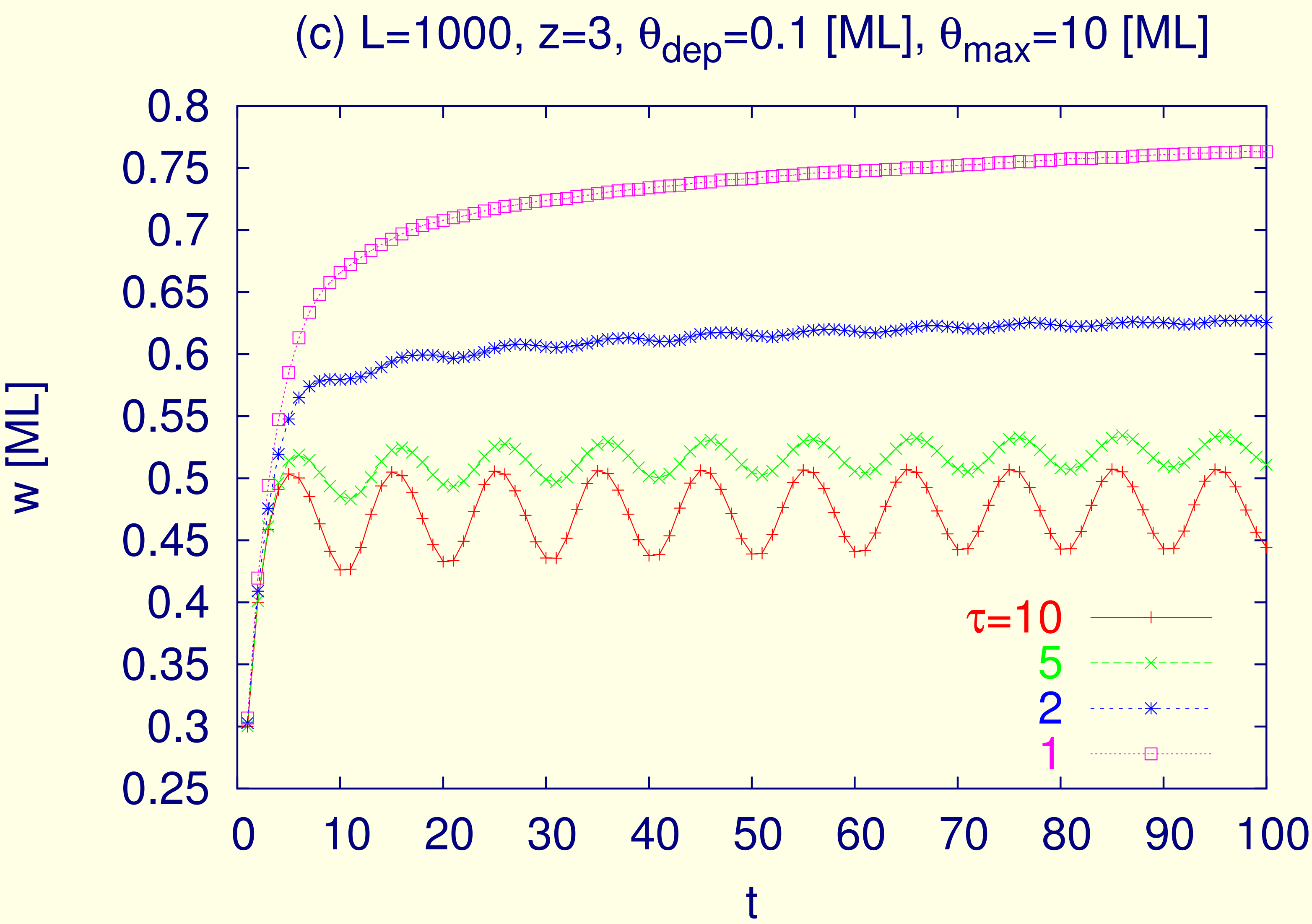

Figure 7: $z = 3$, $L = 10^3$, $\theta_{\mathrm{dep}} = 0.1$ [ML]

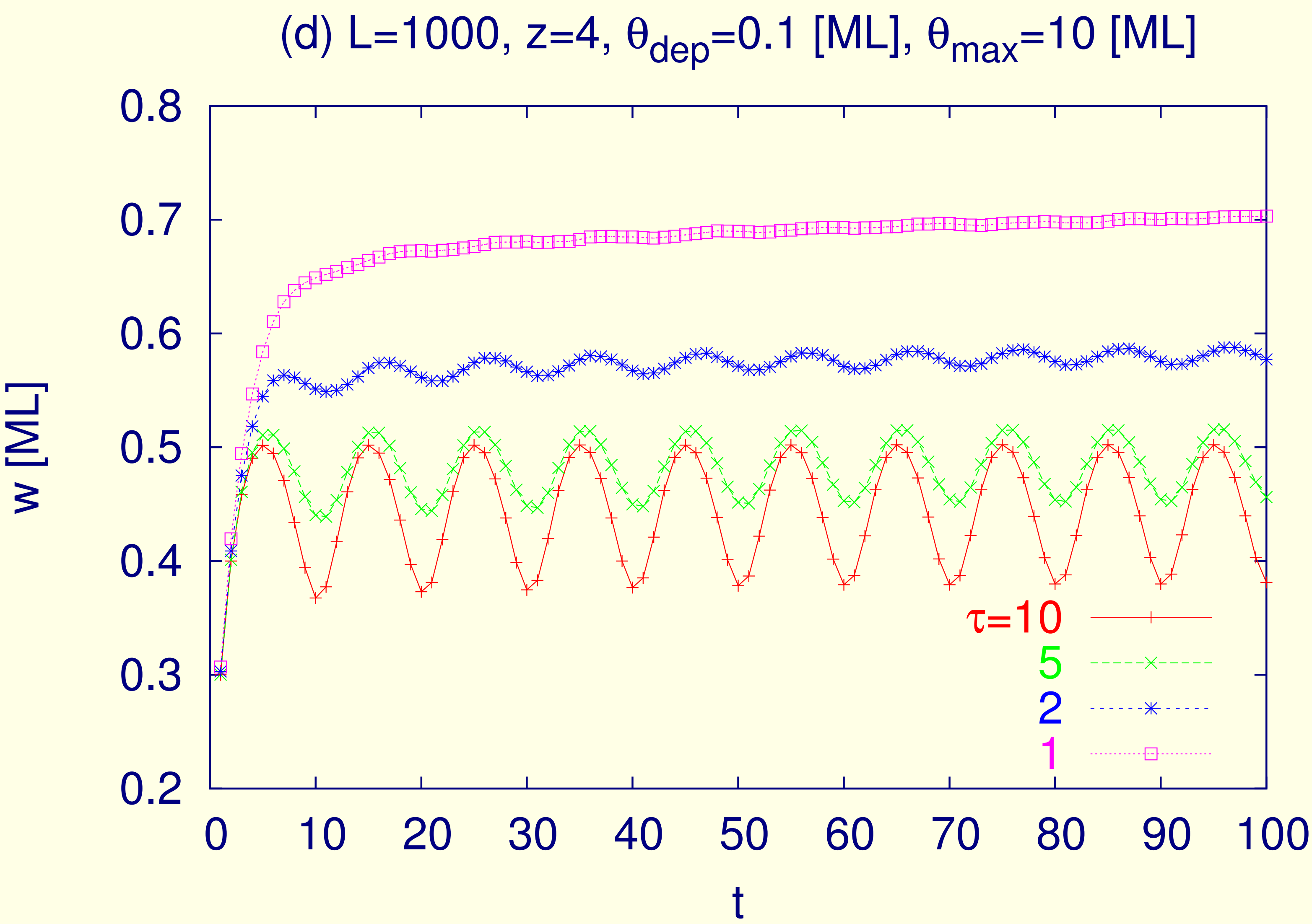

Figure 8: $z = 4$, $L = 10^3$, $\theta_{\mathrm{dep}} = 0.1$ [ML]

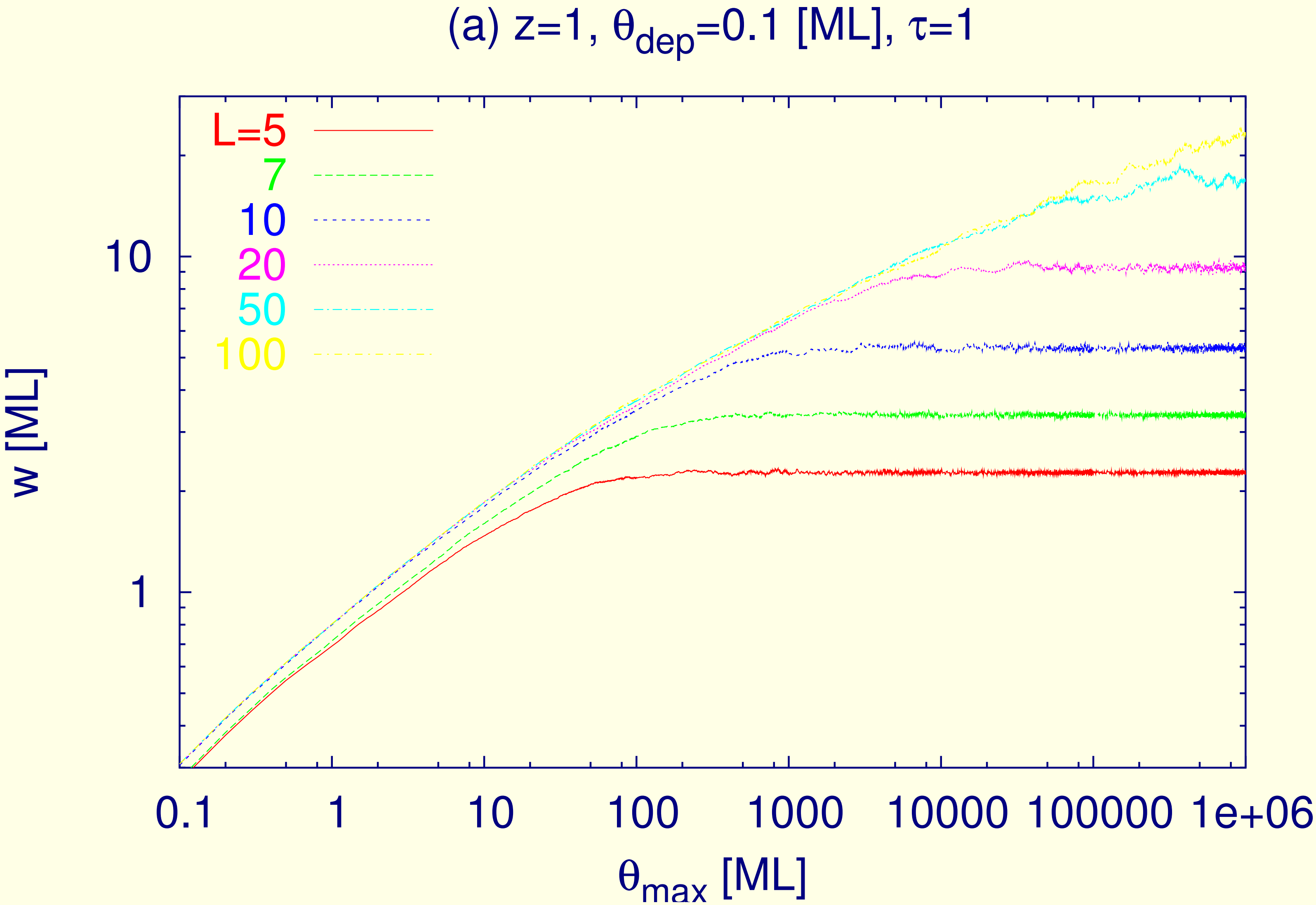

Figure 9: $z = 1$, $\theta_{\mathrm{dep}} = 0.1$ [ML] and $\tau = 1$

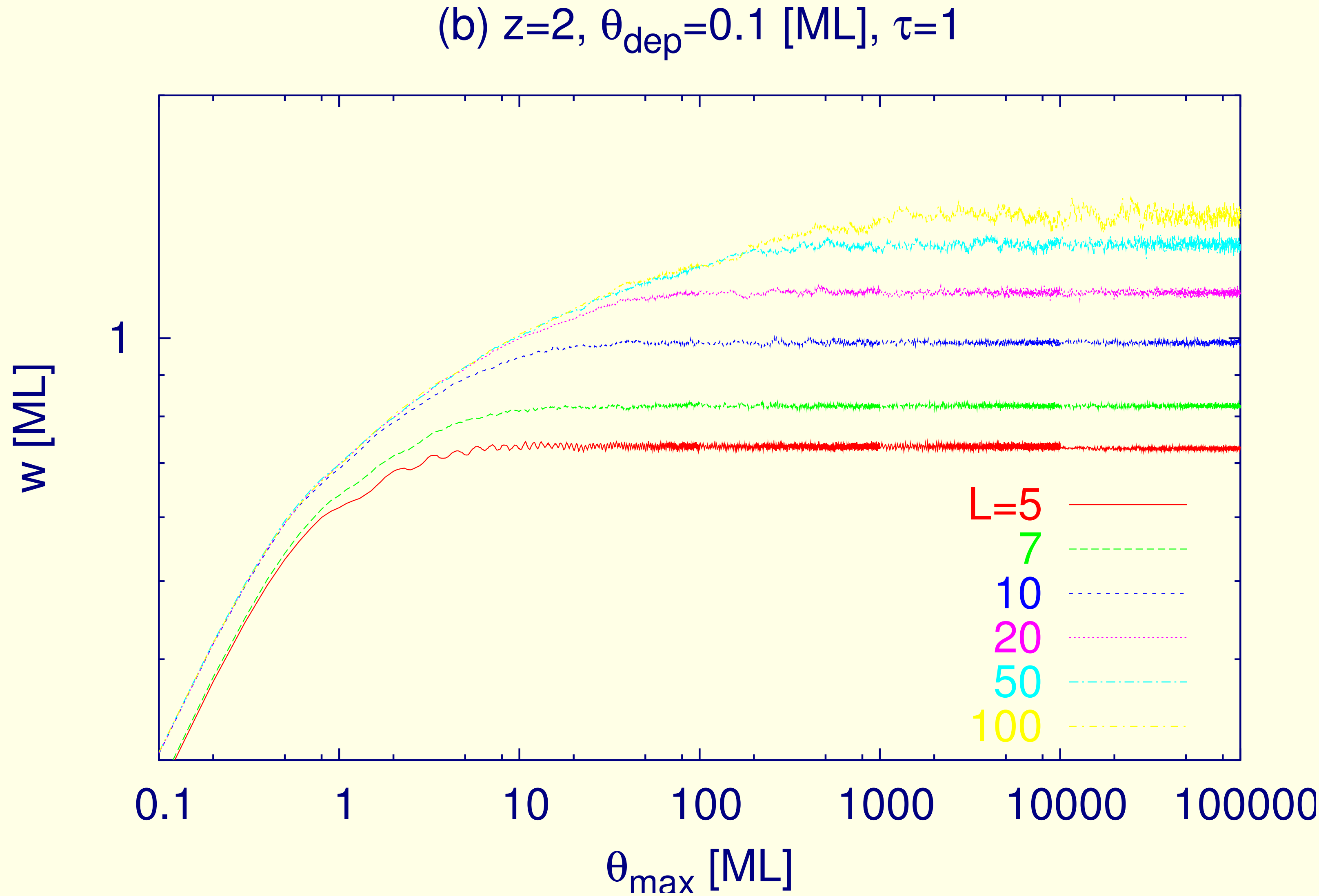

Figure 10: $z = 2$, $\theta_{\text{dep}} = 0.1$ [ML] and $\tau = 1$

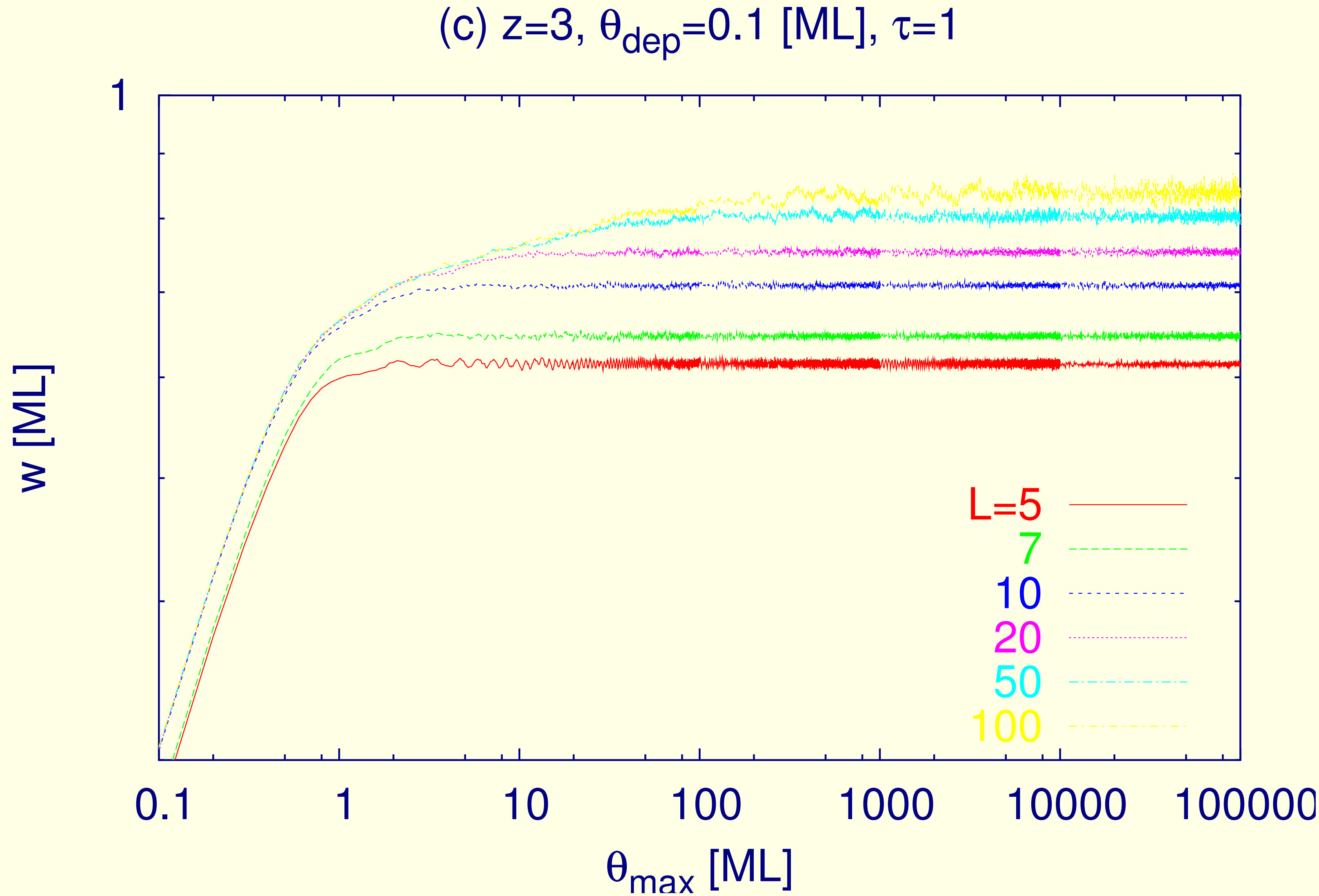

Figure 11: $z = 3$, $\theta_{\rm dep} = 0.1$ [ML] and $\tau = 1$

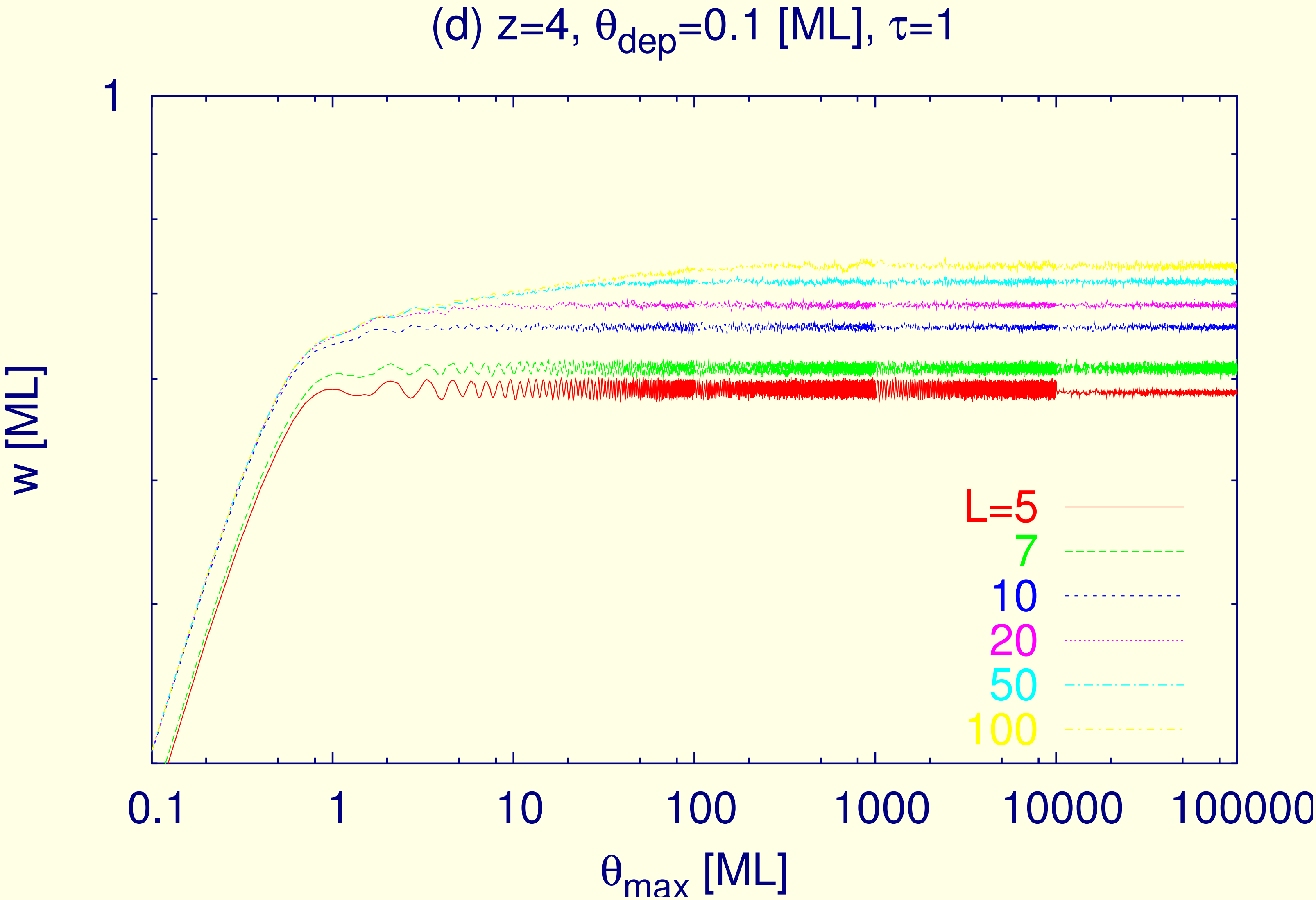

Figure 12: $z = 4$, $\theta_{\text{dep}} = 0.1$ [ML] and $\tau = 1$

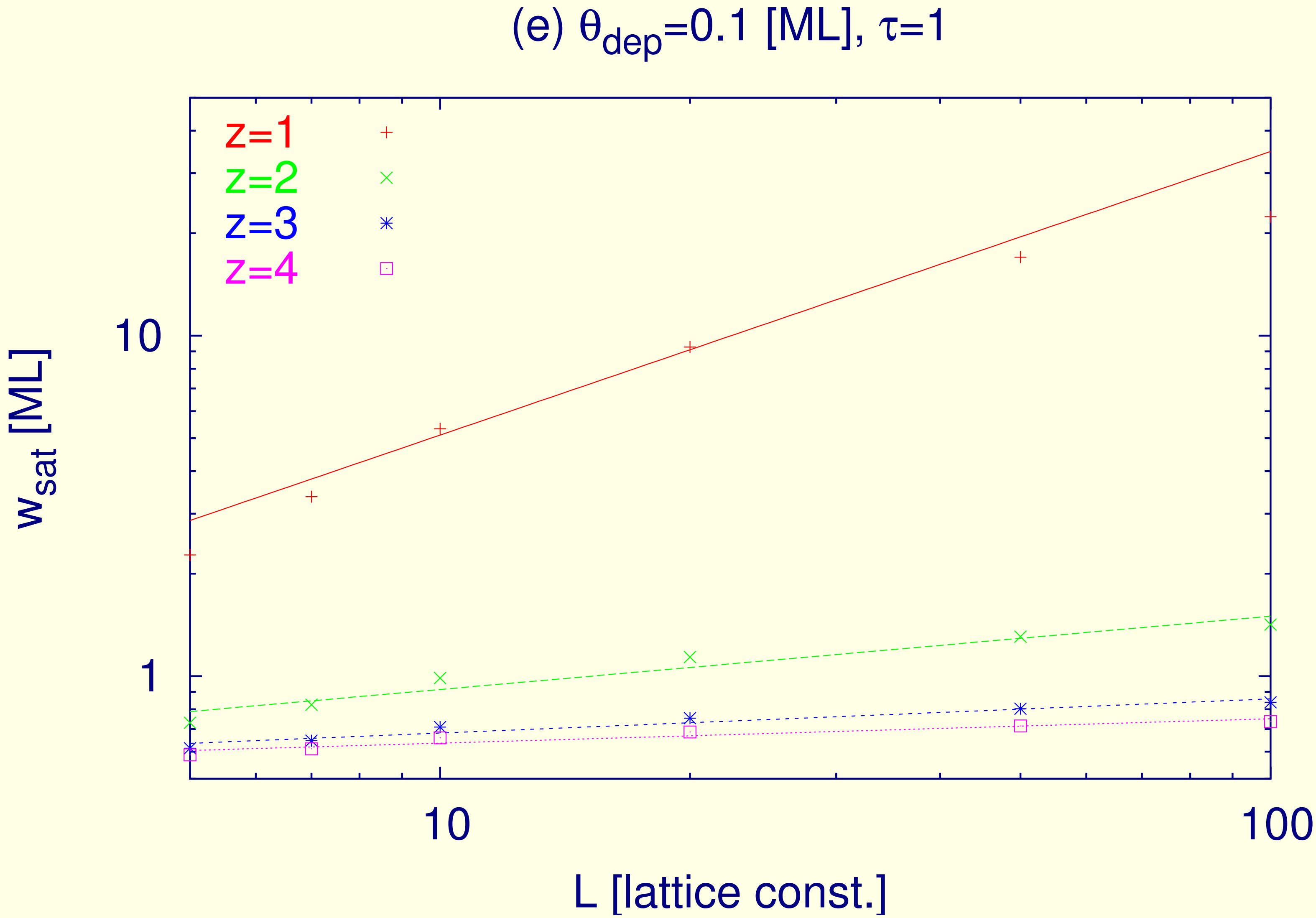

Figure 13: $\theta_{dep} = 0.1$ [ML] and $\tau = 1$

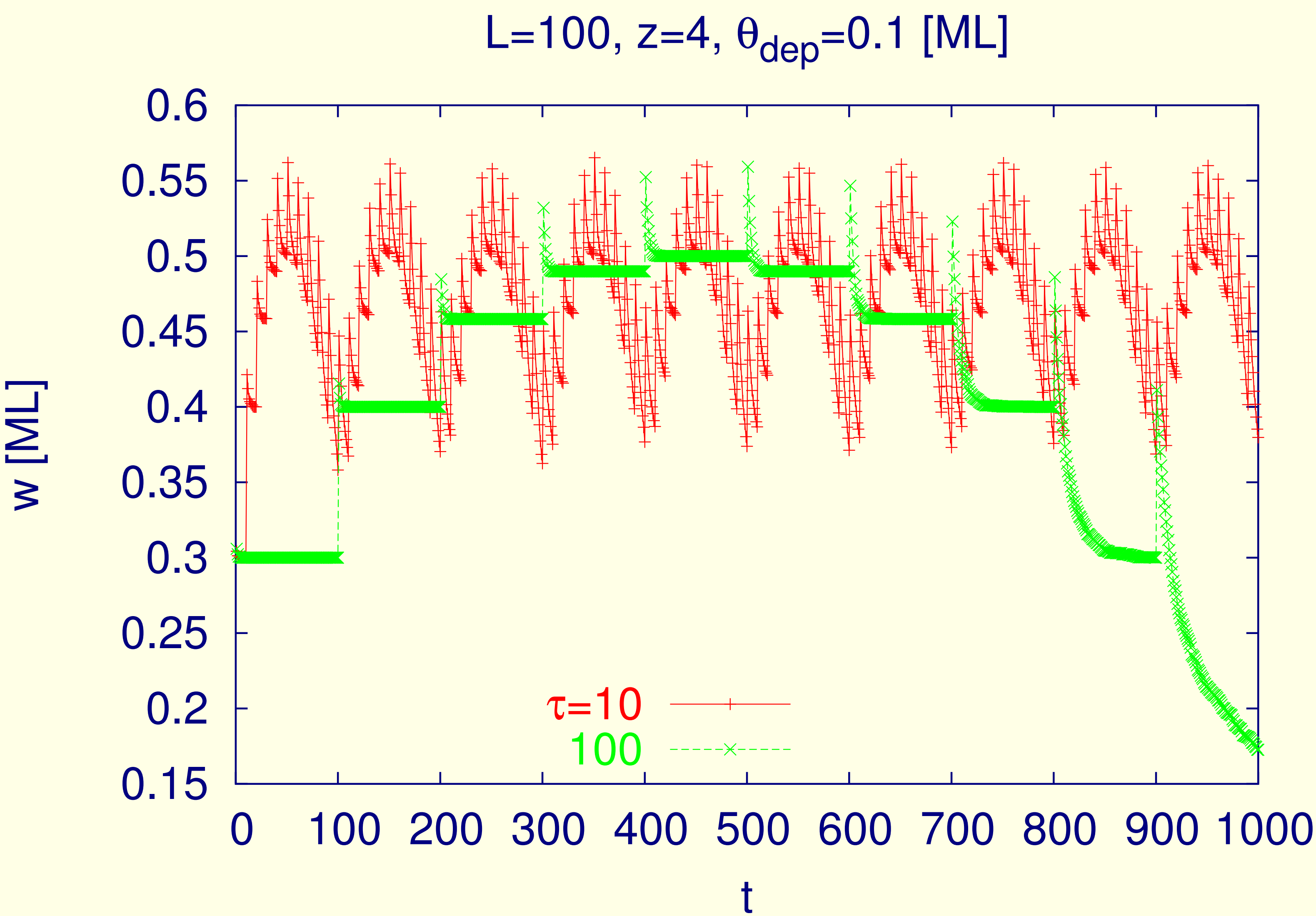

Figure 14: $L = 100$, $z = 4$, $\theta_{\mathrm{dep}} = 0.1$ [ML]

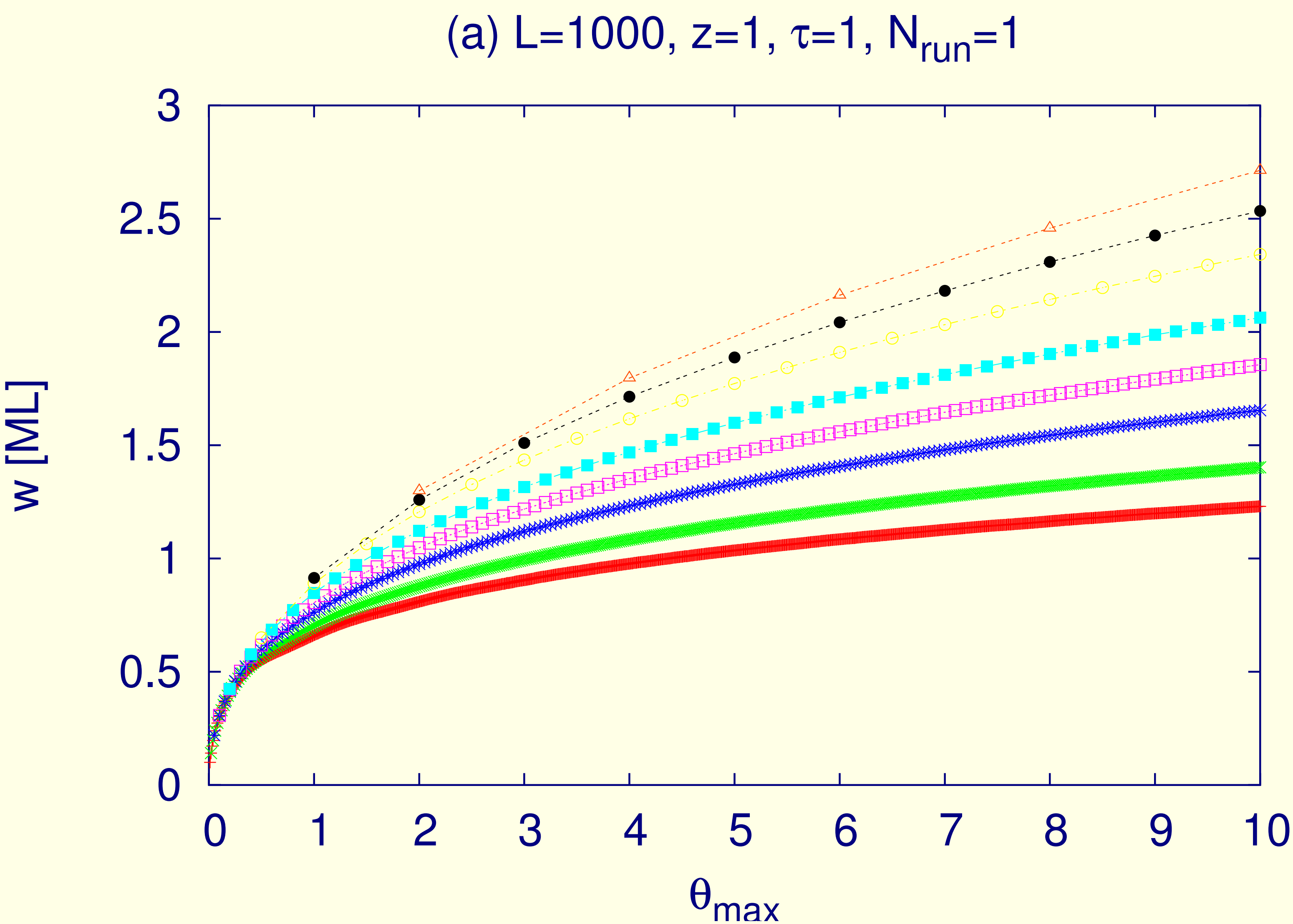

Figure 15: $L = 1000,\ \tau = 1,\ z = 1$ and $\theta_{dep} = 0.01, \cdots, 2.0$ from bottom to top

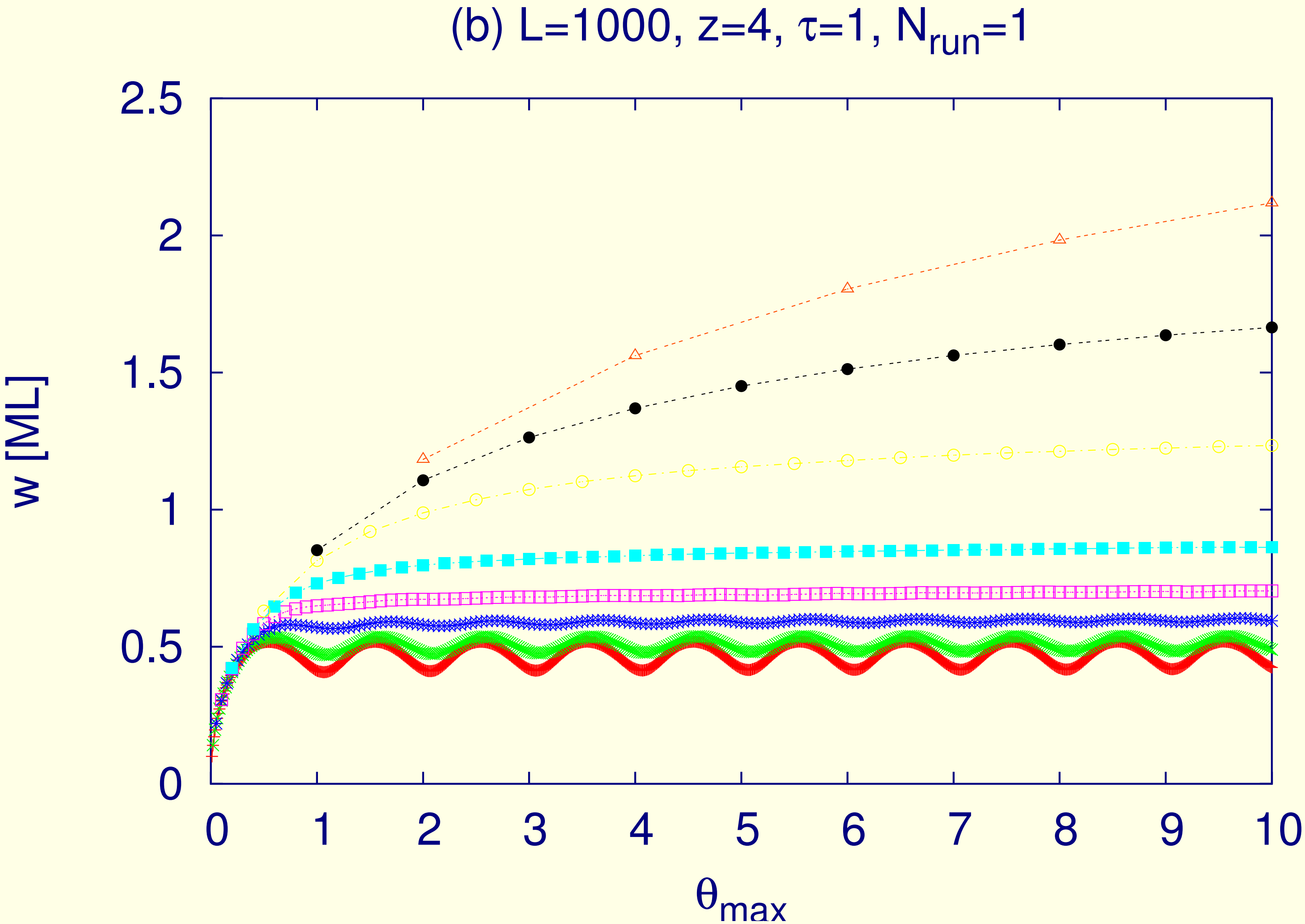

Figure 16: $L = 1000,\ \tau = 1,\ z = 4$ and $\theta_{dep} = 0.01, \cdots, 2.0$ from bottom to top

6.3 Anisotropic growth [10, 12]

The combination of all the information form $G(1,0)$, $G(0,1)$ and $G(1,1)$ is indicative of the type of film morphology, its roughness and anisotropy.

Table 2: $\varepsilon_{1,2,3}$ for different $z_{x,y}$

1	2	1	3	2	3
2	1	3	1	3	2
0.42	-0.42	0.46	-0.46	0.01	-0.01
3.05	0.44	3.32	0.41	1.11	1.04
2.61	2.61	2.61	2.61	3.56	3.56

6.4 Surface selfaffinity

anisotropic case: $J_x \longrightarrow -\infty$, $V_y \longrightarrow \infty$

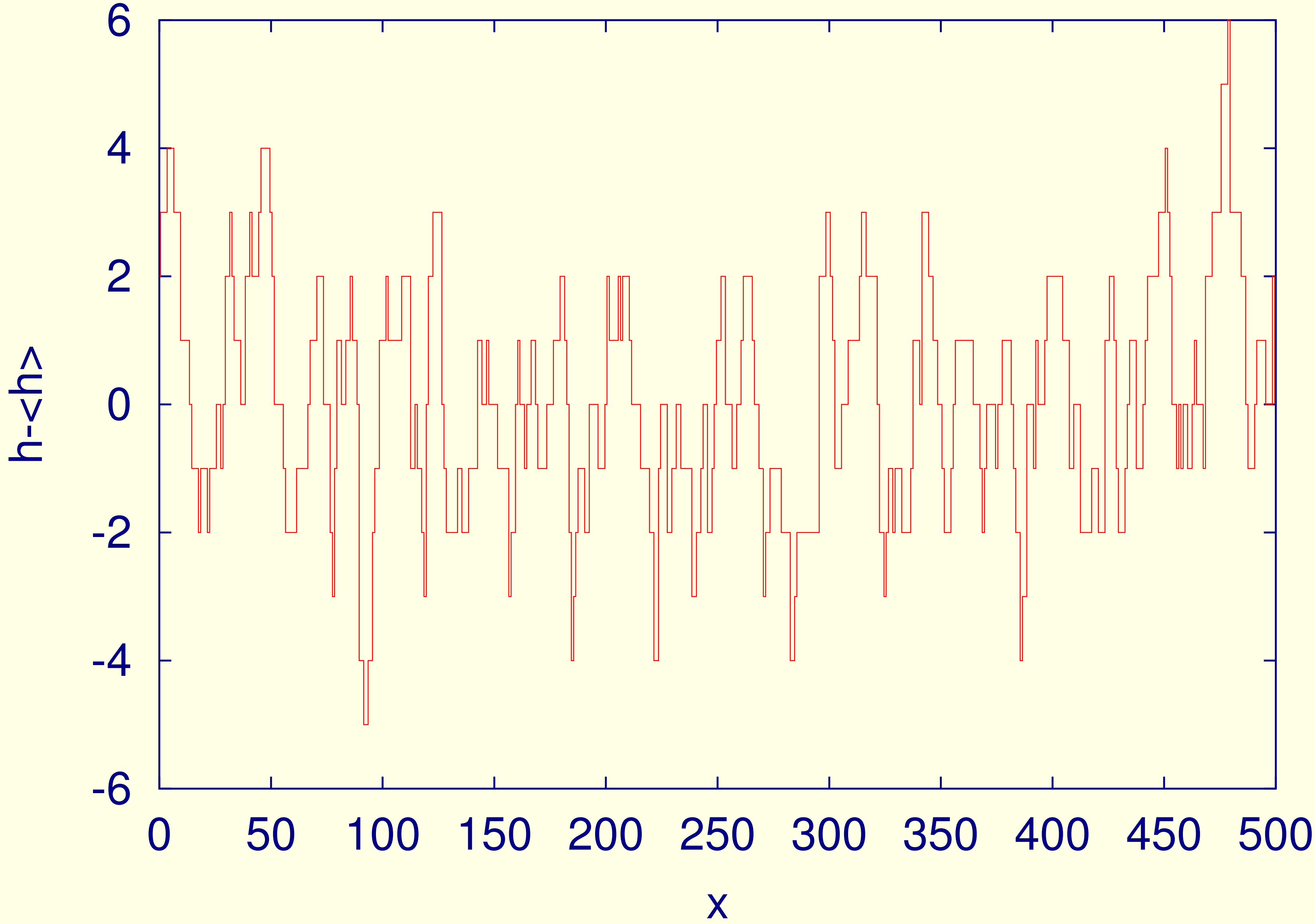

Figure 17: $\langle h \rangle = 2^4$ [ML]

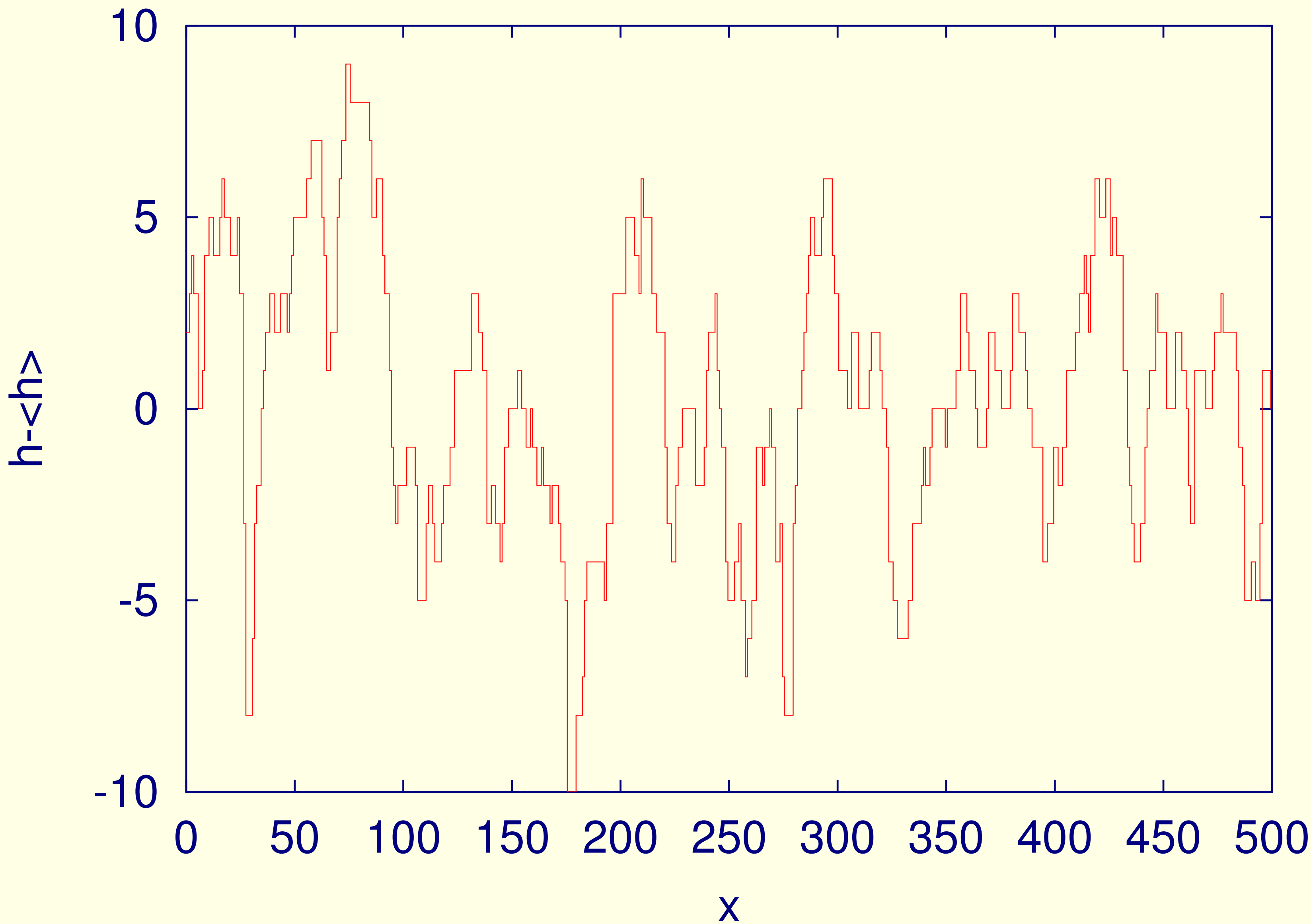

Figure 18: $\langle h \rangle = 2^8$ [ML]

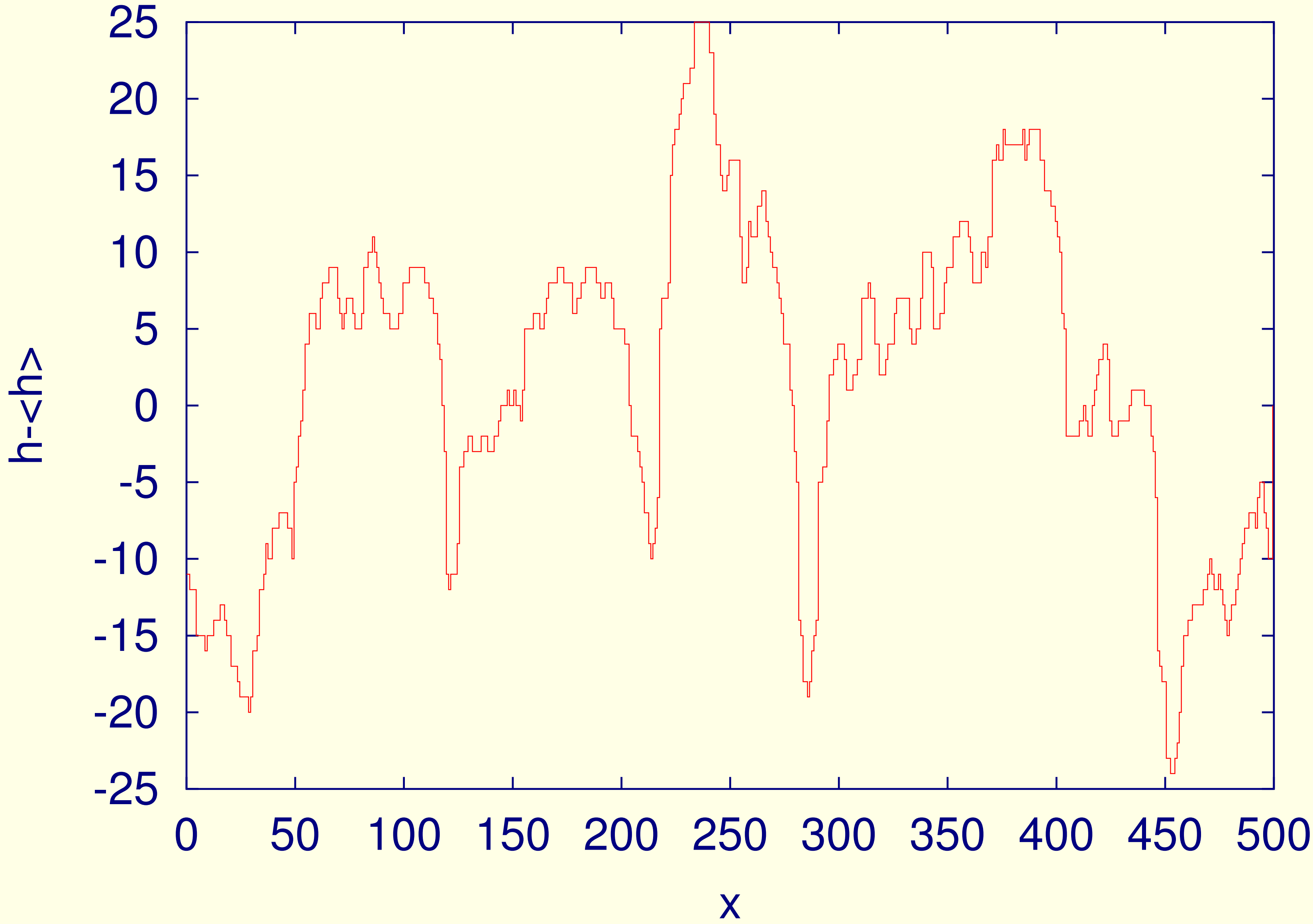

Figure 19: $\langle h \rangle = 2^{12}$ [ML]

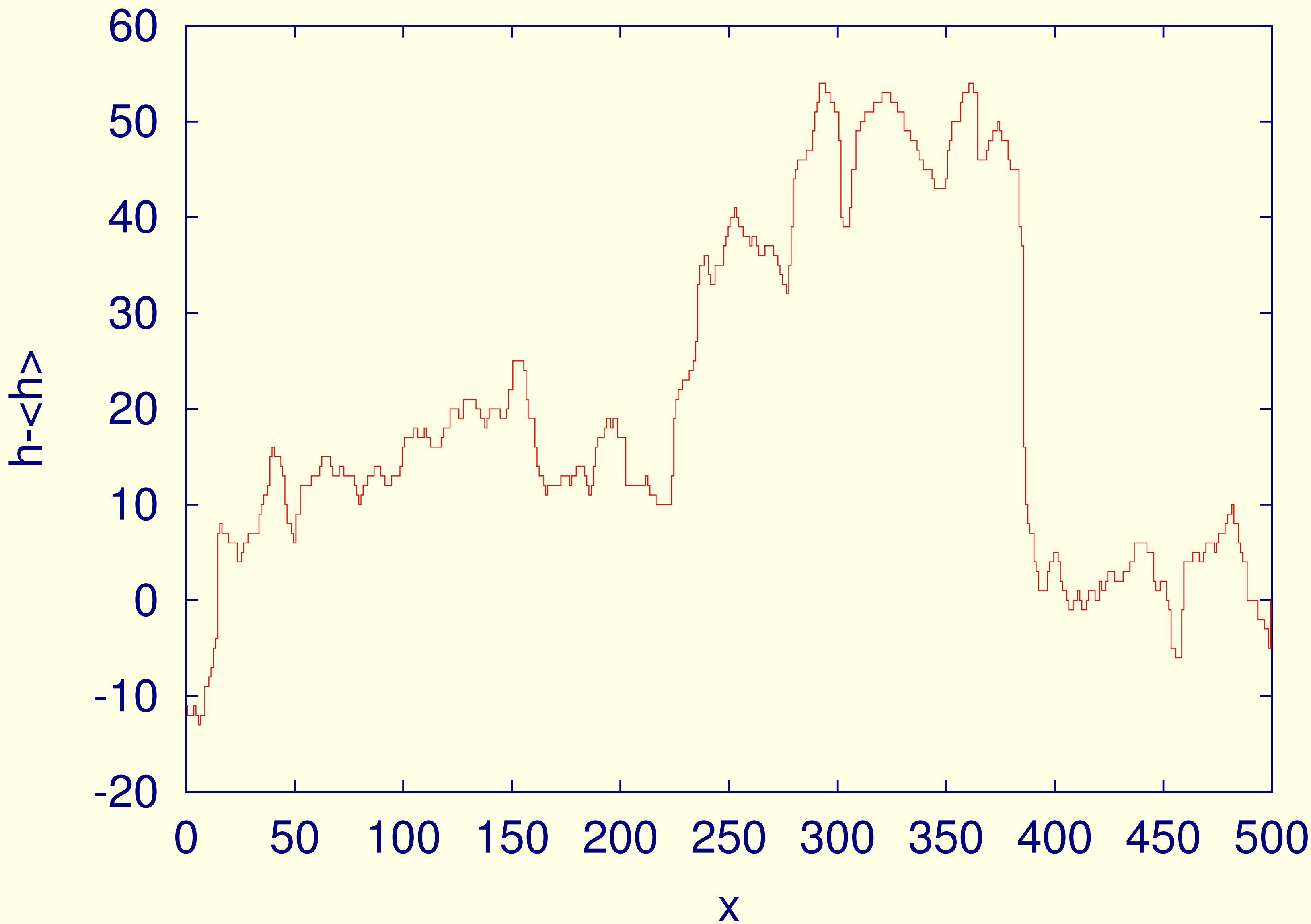

Figure 20: $\langle h \rangle = 2^{16}$ [ML]

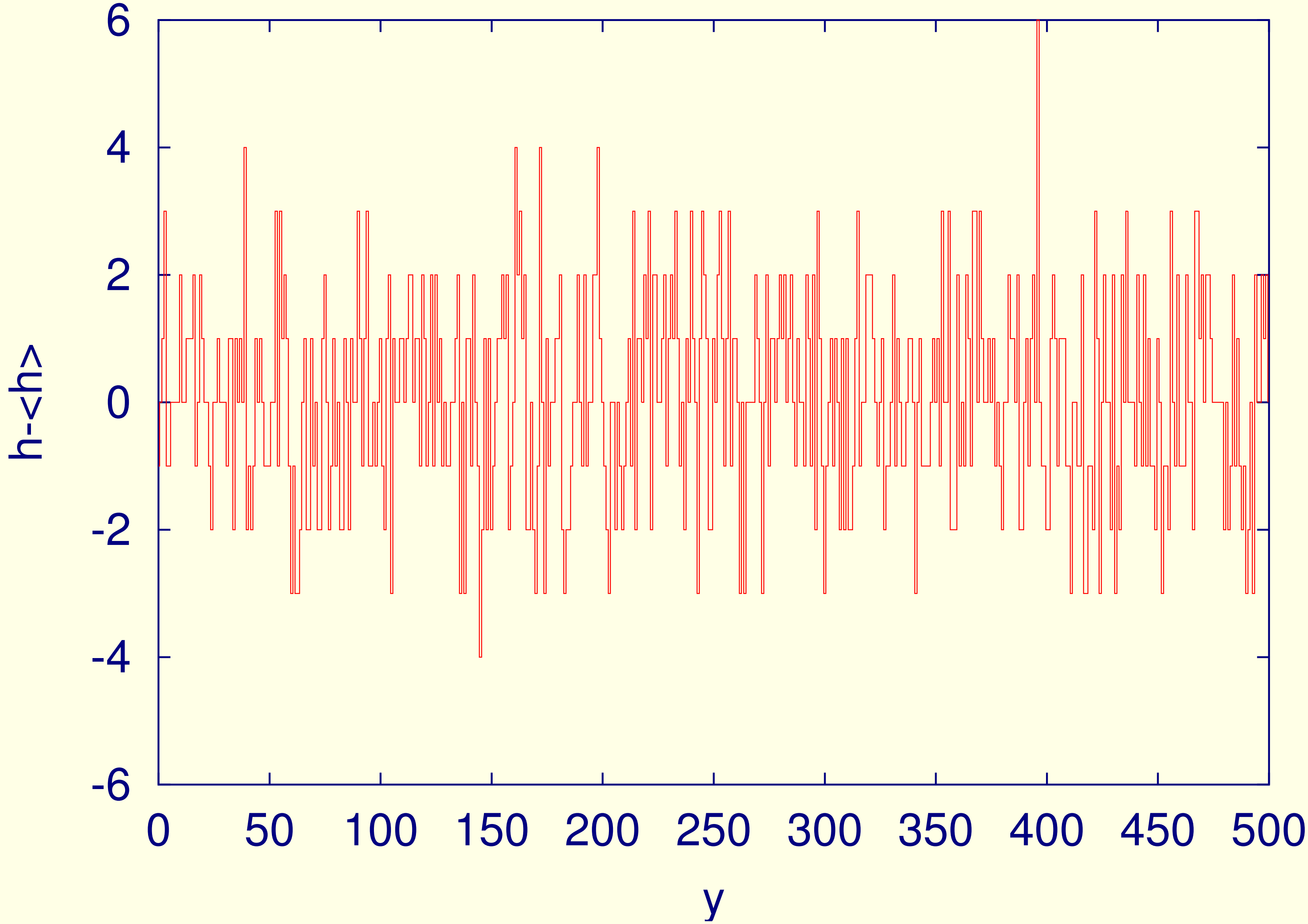

Figure 21: $\langle h \rangle = 2^4$ [ML]

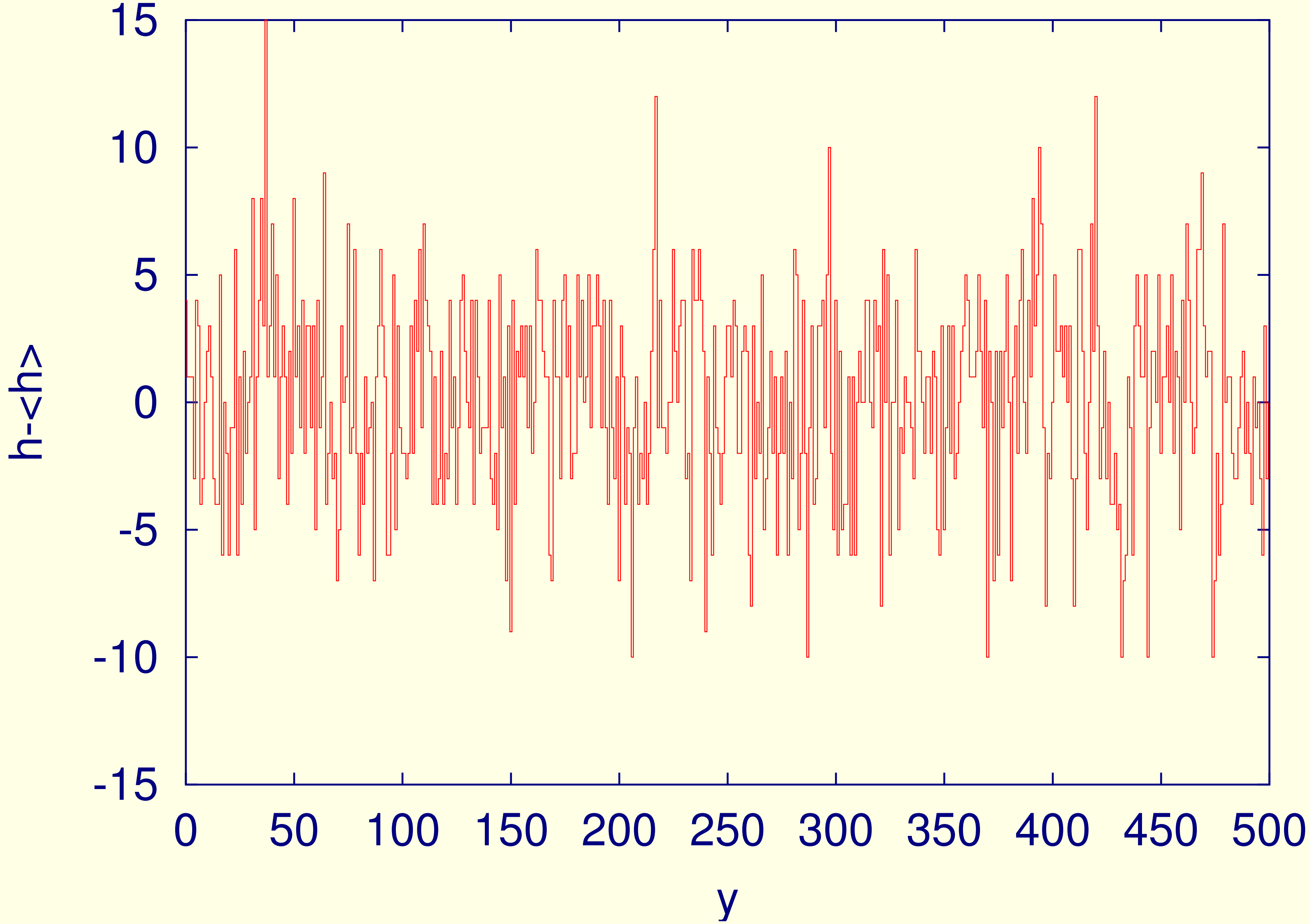

Figure 22: $\langle h \rangle = 2^8$ [ML]

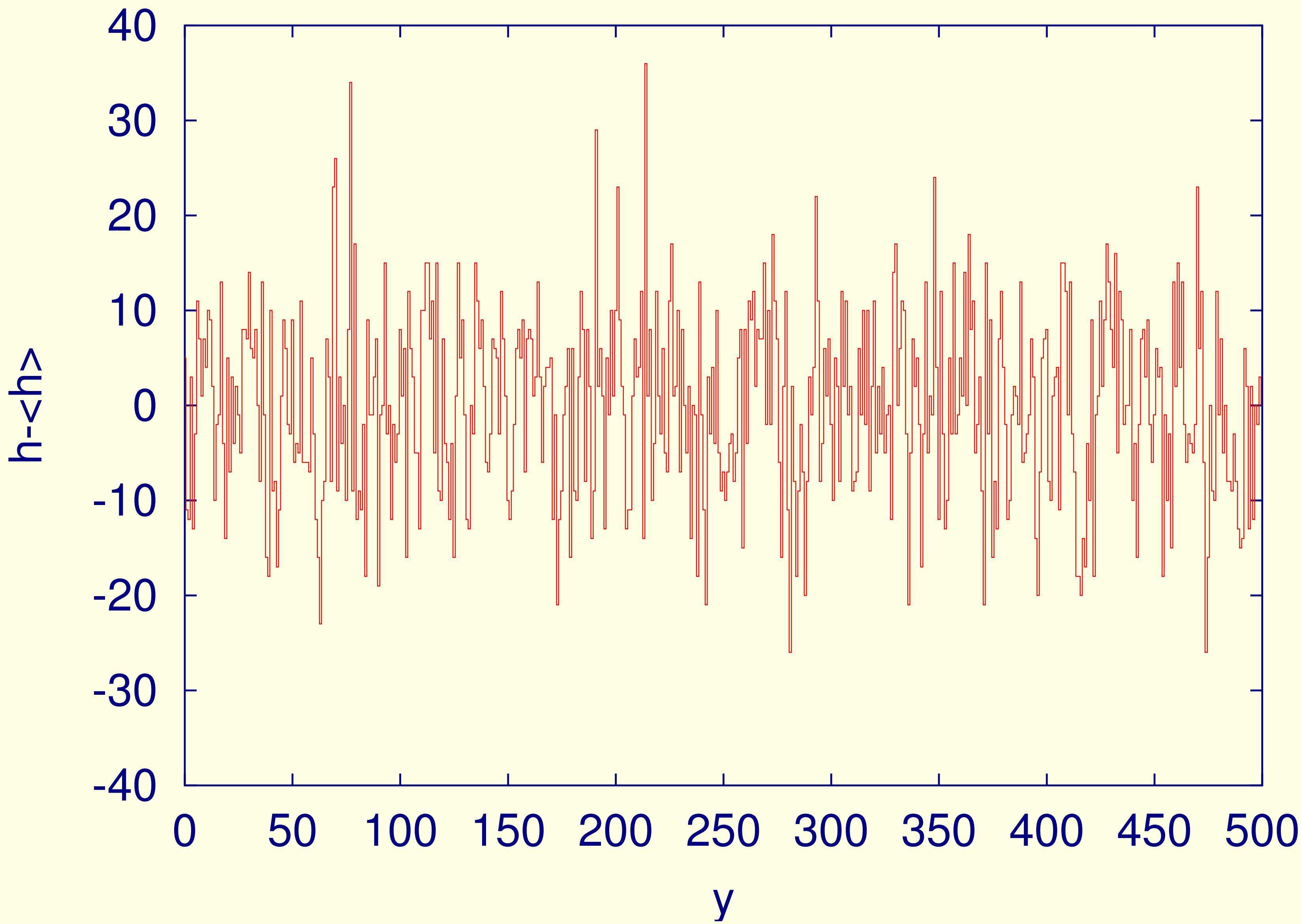

Figure 23: $\langle h \rangle = 2^{12}$ [ML]

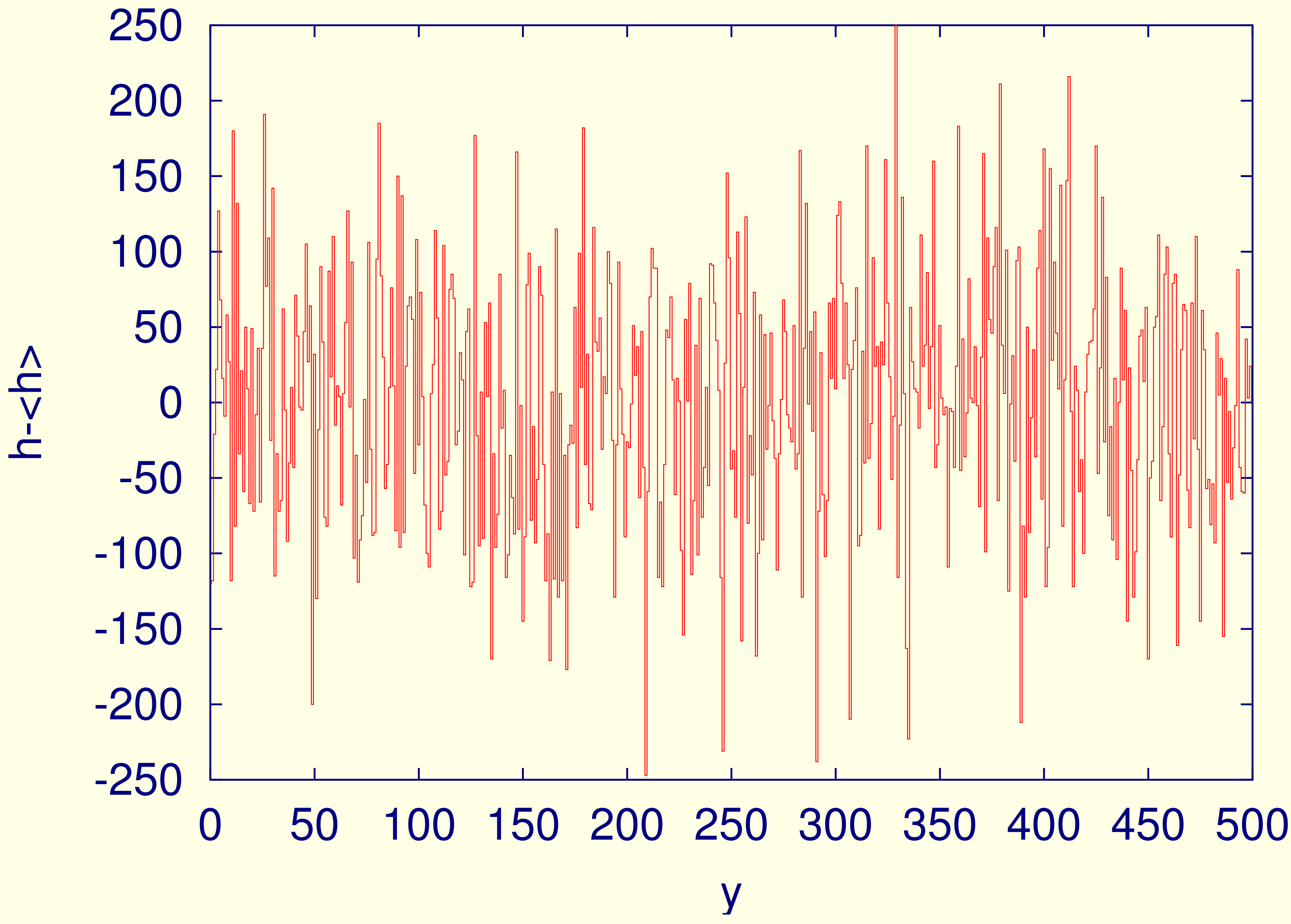

Figure 24: $\langle h \rangle = 2^{16}$ [ML]

Acknowledgements

The machine time on SGI2800 and HP Integrity Superdome in ACK-CYFRONET-AGH is financed by the Polish Ministry of Science and Information Technology.

References

[1] A.-L. Barabási, H. E. Stanley, Fractal concepts in surface growth (Cambridge Univ. Press, 1995)

[2] S. Wolfram, Theory and Applications of Cellular Automata (World Scientific, 1986)

[3] M. A. Herman, Molecular beam epitaxy (Springer, 2000)

[4] M. Prutton, Introduction to surface physics (Oxford Univ. Press, 1986)

[5] F. Family, T. Vicsek, J. Phys. **A18** (1985) L75

[6] F. Family, J. Phys. **A19** (1986) L441

[7] S. Das Sarma, P. Tamborenea, Phys. Rev. Lett. **66** (1991) 325

[8] D. E. Wolf, J. Villain, Europhys. Lett. **13** (1990) 389

[9] K. Malarz, A. Z. Maksymowicz, Int. J. Mod. Phys. **C10** (1999) 645

[10] K. Malarz, A. Z. Maksymowicz, Int. J. Mod. Phys. **C10** (1999) 659

[11] K. Malarz, Int. J. Mod. Phys. **C11** (2000) 1561

[12] R. Kosturek, K. Malarz, Physica **A** — in print.